Supplementary S1: Methods

S1.1 Observational Constraint on Arctic Amplification Supplementary

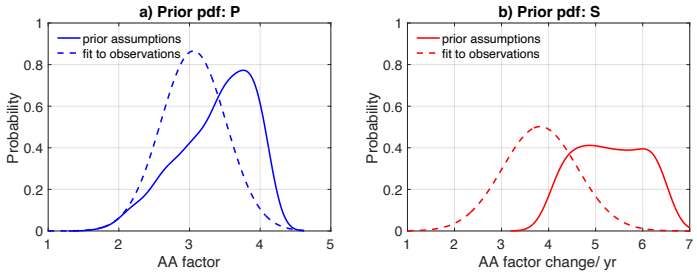

Figure S1. Contribution of each parameter to the observationally constrained Arctic Amplification between 1970 and 2100. a and b) show the two initial distributions for parameters s and p before they are averaged and normalised. The solid line reflects our assumptions of current and future Arctic Amplification, while the dashed line reflects actual trends from both observations and CMIP6 models.

We generate values for s and p by averaging two distributions for each parameter (fig. S1a-b). The Bayesian nature of our approach allows us to inform our routine with expert judgement, the first distribution is generated from our assumptions of future and current Arctic Amplification trends. Whereas the second is informed from observational and CMIP6 data. This approach considers CMIP6 data and observations while accounting for the uncertain future of Arctic Amplification due to model biases. For p we first generate a right skewed poisson distribution that applies a greater weight to higher Arctic Amplification possibilities, as it is plausible that Arctic Amplification will continue to increase into the future given observed trends (Rantanen et al. (2022); Chylek et al. (2022)). The amplification factor is also physically unlikely to be less than one as this would cause the Arctic to warm at a slower rate than the global mean. For s, we generate a uniform distribution, as the observational datasets used in this analysis suggest that the rate of increase in Arctic Amplification per degree of warming is generally uniformly spread across its range. The second distribution describes the probability of s and p based on available observational and model data. For p, we generate a Gaussian distribution from the standard deviation and mean of the average 2012-2100 CMIP6 Arctic Amplification. Similarly, we set up the second distribution for s by generating a Gaussian distribution from the mean and standard deviation of the observed rate of Arctic Amplification increase with global warming. We then average and normalise the two distributions for each parameter to generate a single distribution (fig. 3c-d). Our resultant p distribution follows a right skewed distribution with a broad peak ranging between 3.5 and 3.8. Whereas our s distribution is a simple normal distribution about 4.8. This process aims to derive a more realistic description of the key features of Arctic Amplification evolution through distributions informed from observations, models and our best understanding of future trends. We randomly sample values from the final distributions of s, p and r and input these values into Eq. (1), to generate the constrained range of probabilistic Arctic Amplification projections shown in figure 3.

To generate the Arctic annual temperature anomaly, we multiply 'r' with a randomly sampled Arctic Amplification ensemble member. To convert the anomalies into absolute temperatures, we add the mean 1850-1900 observed absolute Arctic annual temperature to our emulated anomaly projections. We iteratively repeat this process to generate a 600-ensemble member Arctic annual mean temperature ensemble, which is input into our seasonal temperature parameterisation in the next step (step ii).

S1.2 Additional Figures: CMIP6 Calibration

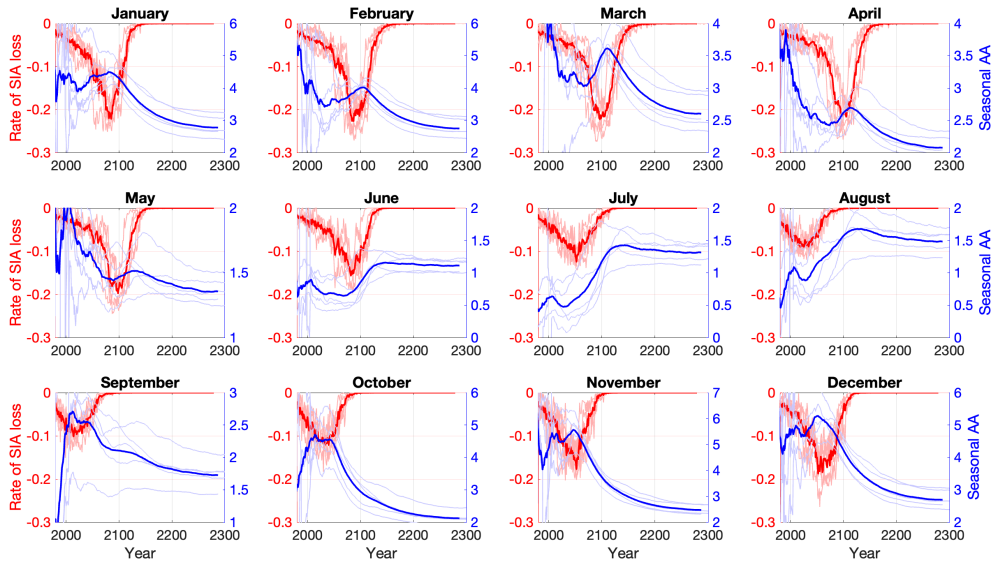

Figure S2. Comparison of the seasonal Arctic Amplification with the rate of SIA loss to 2300. Dark red lines show the mean rate of sea ice loss in each month per year, while lighter red lines show the rate from each of the 5 models used in this analysis. The rate is calculated here as the difference in SIA between each year for each month. Dark blue lines show the mean Arctic Amplification evolution to 2300 in each month, while lighter blue lines show the temperature amplification in each model. The seasonal Arctic Amplification is calculated from the division of the seasonal Arctic temperature by the global mean temperature.

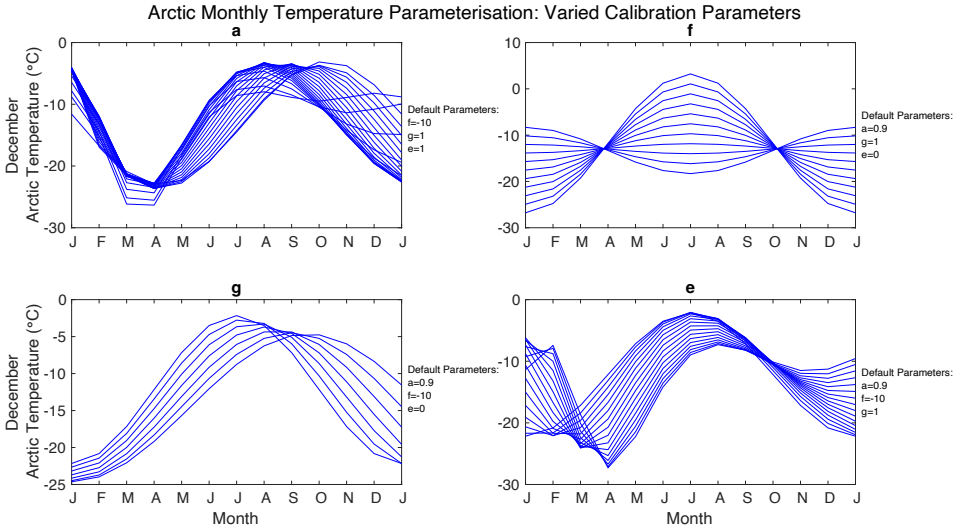

Figure S3. Visualisation of the role of each calibration parameter in our seasonal Arctic temperature parameterisation (Eq. 2b). Each box denotes the evolution of each calibration parameter in our seasonal temperature parameterisation, and how they change with annual temperature. All other parameters in each parameterisation are kept at default values while the parameter of note is varied with temperature.

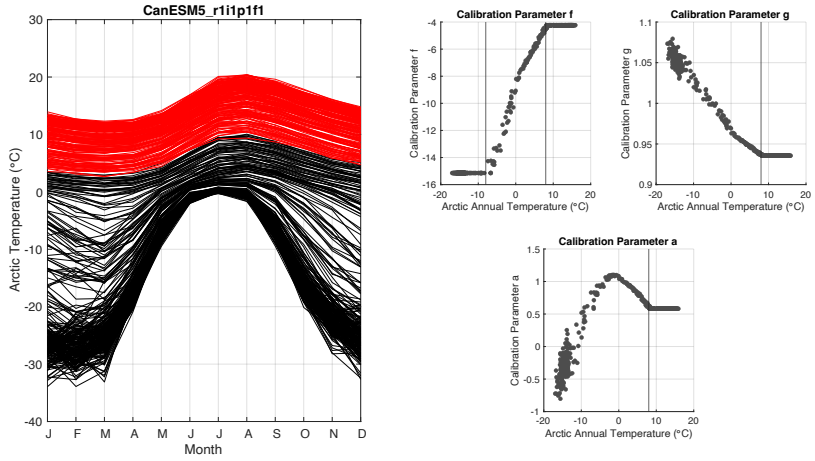

Figure S4. CMIP6 Arctic seasonal temperature cycle 1850-2300. Black lines indicate the 1850-2100 period, while red lines indicate the 2100-2300 period, highlighting the lack of change in shape of the Arctic seasonal temperature cycle after 2100. Box a-c show the temperature dependence of calibration parameters f, g and a, where grey vertical lines indicate the lack of change in these parameters after the Arctic annual temperature reaches 6°C, where they are forced to remain constant with changes to the Arctic annual temperature to prevent further change to the emulated seasonal cycle. The second grey vertical line in the calibration parameter 'f' box indicates the Arctic annual temperature 'f' is forced to remain constant until to allow summer temperatures to increase at a similar rate to the observed.

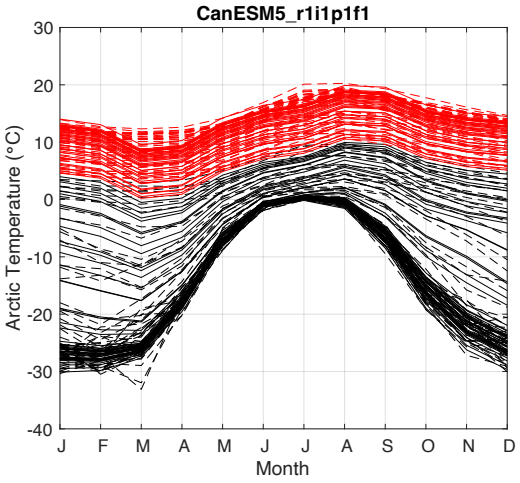

Figure S5. Comparison of our emulated seasonal Arctic temperature evolution with its CMIP6 counterpart to 2300. Black lines represent the 1850-2100 temperature cycle, while red lines represent the 2100-2300 seasonal cycle temperature evolution. Solid lines represent our emulation of the CMIP6 trend, while dashed lines represent CMIP6 data for the first ensemble member of model CanESM5.

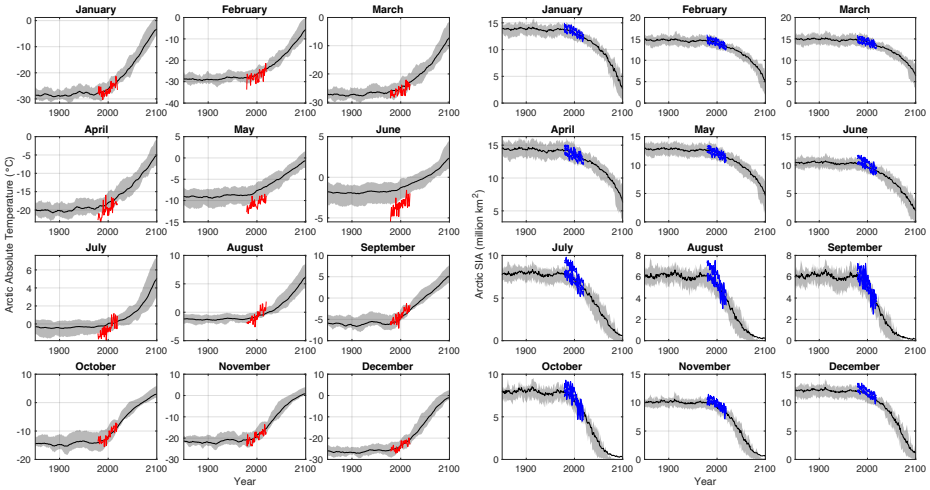

Figure S6. Timeseries of the mean 1979-2014 summer Arctic temperature and SIA bias between CMIP6 models and observations. Shading represents the CMIP6 17th-83rd (*likely*) percentile range, while black lines represent the mean. Left) Arctic monthly surface temperature, observations in red. Right) SIA observations in blue.

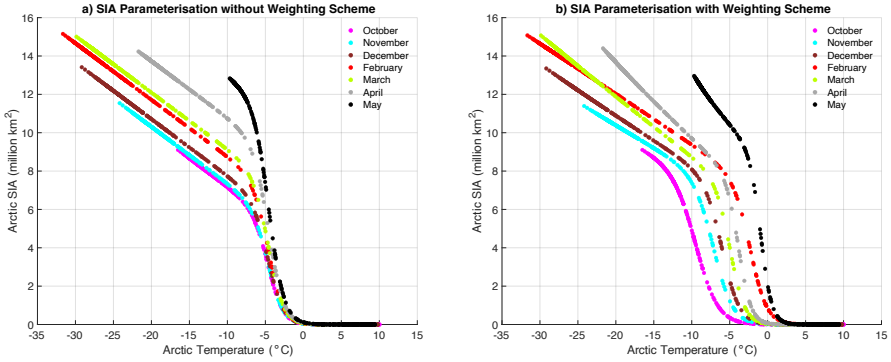

Figure S7. Effect of the weighting scheme on our SIA parameterisation. a) Projections of SIA loss with Arctic warming between October and May without a weighting scheme applied to our SIA parameterisation. b) Projections from the same model as a) when the weighting scheme has been applied. We highlight the warmer temperature of rapid sea ice loss in the melt season than in the growth season.

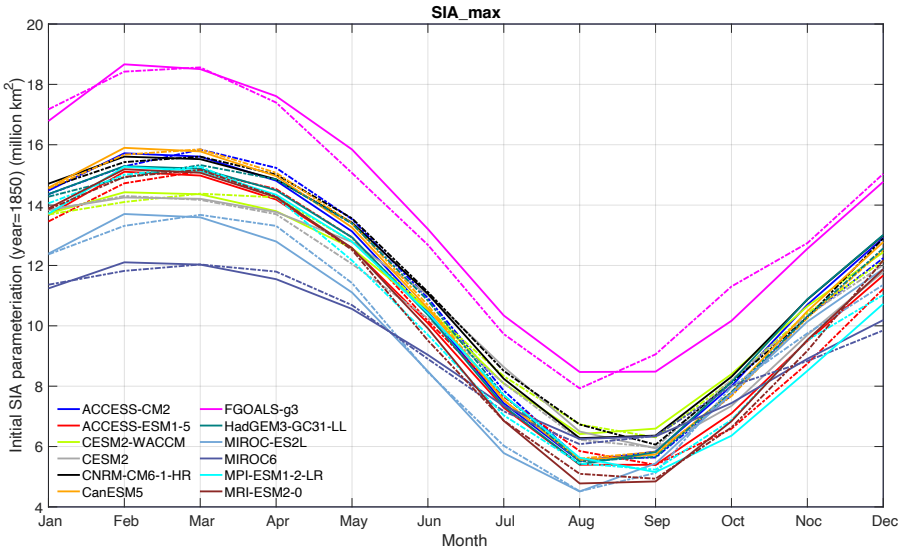

Figure S8. Comparison of our CMIP6 calibrated starting SIA parameter (SIA$_{max}$, Eq: 3c) with its CMIP6 counterpart. Dashed lines represent our calibrated SIA in each month while solid lines represent their CMIP6 counterpart. Each colour represents each of the 12 CMIP6 models used in this study.

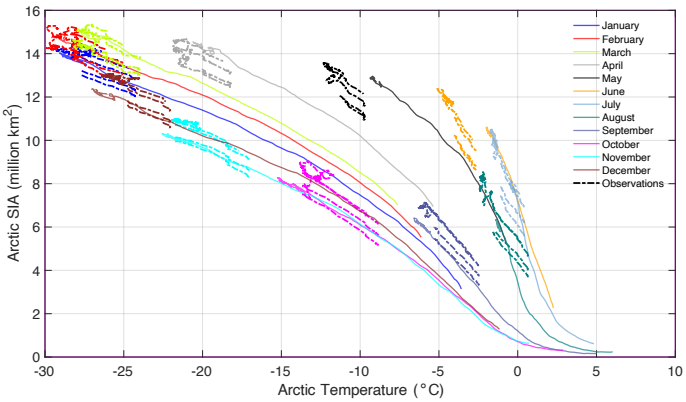

Figure S9. Comparison of the mean CMIP6 SIA as a function of the mean CMIP6 Arctic warming in each month with observations. Showing the higher sensitivity of SIA loss to summer Arctic warming in CMIP6 models than observations. Solid lines represent the CMIP6 mean data in each month and dotted lines represent observations.

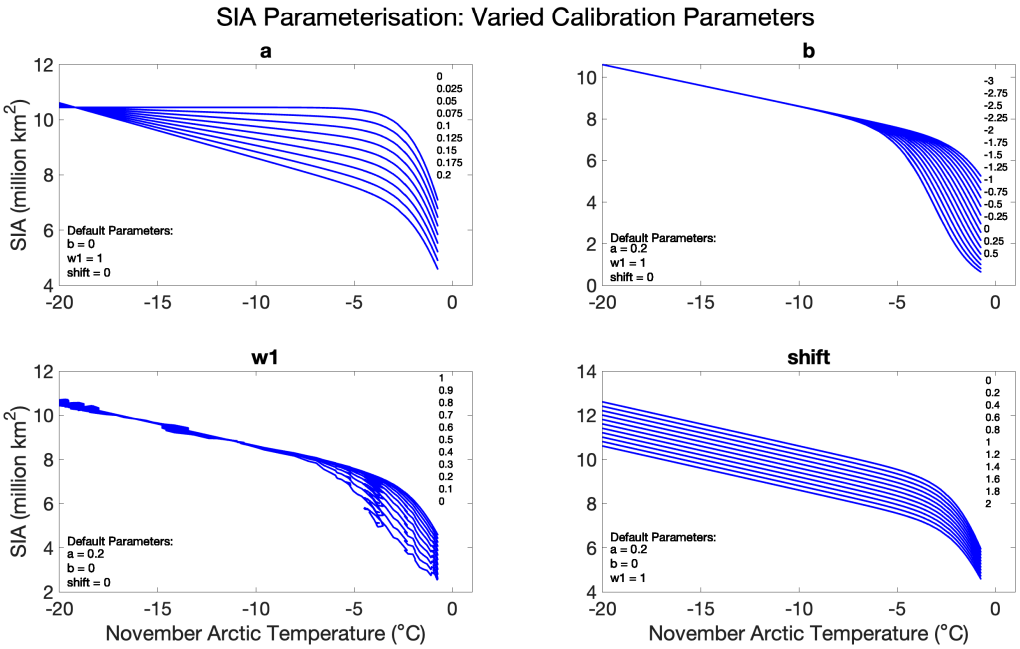

Figure S10. Visualisation of the role of each calibration parameter in our SIA parameterisation (Eq: 5). Each box denotes the evolution of each calibration parameter in our SIA parameterisation, and how they change with temperature. All other parameters in each equation are kept at default values while the parameter of note is varied with temperature.

S1.3 Supplementary Tables

Model Names	$f1$	$f2$	$g1$	$g2$	$a1$	$a2$	$a3$
ACCESS-CM2	0.49	-8.43	-0.0063	0.931	-0.07	-0.58	0.10
ACCESS-ESM1-5	0.56	-7.16	-0.0071	0.93	-0.03	0.14	0.13
CESM2-WACCM	0.63	-6.08	-0.0031	0.97	-0.09	-0.63	0.11
CESM2	0.58	-6.29	-0.0042	0.96	-0.09	-0.64	0.11
CNRM-CM6-1-HR	0.42	-7.78	-0.0007	0.97	-0.06	-0.08	0.13
CanESM5	0.54	-7.47	-0.0076	0.95	-0.09	-0.32	0.01
FGOALS-g3	0.35	-11.4	-0.0009	1.03	-0.01	0.64	0.36
HadGEM3-GC31-LL	0.49	-8.33	-0.0062	0.94	-0.09	-0.54	0.07
MIROC-ES2L	0.45	-9.01	-0.0040	0.98	-0.09	-0.45	0.08
MIROC6	0.44	-8.09	-0.0057	0.95	-0.11	-0.37	0.09
MPI-ESM1-2-LR	0.56	-6.48	-0.0016	0.99	-0.02	0.94	0.57
MRI-ESM2-0	0.52	-7.35	-0.0036	0.96	-0.09	-0.50	0.09

Table S1. Arctic seasonal parameterisation (step ii, Eq: 2b) calibration results with parameter sets for the available 12 CMIP6 models. Calibration parameters are introduced in Section 2.4. The mean response of the calibration data is given at the bottom of the table.

Model Names	a	d	$w1$	b
ACCESS-CM2	0.38	0.39	0.54	-1.32
ACCESS-ESM1-5	0.40	-0.04	0.55	-0.98
CESM2-WACCM	0.29	0.06	0.21	-4.44
CESM2	0.29	-0.13	0.13	-4.43
CNRM-CM6-1-HR	0.41	-0.01	1.00	-0.77
CanESM5	0.40	0.54	0.55	0.66
FGOALS-g3	0.35	-0.14	0.45	0.65
HadGEM3-GC31-LL	0.32	0.45	0.27	-0.99
MIROC-ES2L	0.32	-0.47	0.49	-1.11
MIROC6	0.26	0.20	0.00	-1.36
MPI-ESM1-2-LR	0.39	-0.44	0.00	-1.71
MRI-ESM2-0	0.38	0.09	0.19	-1.83

Table S2. SIA parameterisation (step iii, Eq: 3b) calibration results with parameter sets for the available 12 CMIP6 models. Calibration parameters are introduced in Section 2.5. The mean response of the calibration data is given at the bottom of the table.

Months	**AMST: Standard Deviation**		**AMST: Mean**	
	CE: Emulation	CMIP6	CE: Emulation	CMIP6
January	5.58	5.74	-19.2	-18.5
February	5.51	5.55	-20.4	-20.4
March	4.68	4.88	-20.9	-19.6
April	3.57	3.75	-15.8	-5.08
May	2.43	2.61	-6.50	-4
June	1.65	1.36	-0.48	-0.19
July	1.41	1.02	0.99	0.93
August	1.75	1.77	1.53	1.03
September	2.82	3.18	-0.56	-0.43
October	4.51	5.21	-5.24	-3.67
November	6.25	6.19	-9.04	-8.73
December	7.02	6.28	-13.5	-14.6
Mean	**3.93**	**3.96**	**9.09**	**-8.61**

Table S3. Table of the mean and standard deviation of the average 2080-2100 emulated (CE) Arctic seasonal temperature (AMST) multi-model range in each month. (I extract the 2080-2100 range in model, find the mean in each model, and then calculate the mean and std across all of the models to find the multi-model mean and std). All values are rounded to three significant figures.

Months	**SIA: Standard Deviation**		**SIA: Mean**	
	CE: Emulation	CMIP6	CE: Emulation	CMIP6
January	1.83	1.69	9.10	10.8
February	1.78	1.58	11.3	12.1
March	1.68	1.51	12.1	12.4
April	1.49	1.45	11.8	11.9
May	1.26	1.49	10.9	10.3
June	1.52	1.74	8.24	7.77
July	2.09	2.16	3.49	4.36
August	1.89	2.10	2.00	1.99
September	2.09	2.07	1.33	1.51
October	2.34	2.42	2.36	2.76
November	1.75	2.31	5.23	5.57
December	1.83	1.83	7.12	8.77
Mean	**1.79**	**1.86**	**7.09**	**7.53**

Table S4. Table of the mean and standard deviation of the average 2080-2100 emulated (CE) SIA multi-model range in each month. (I extract the 2080-2100 range in model, find the mean in each model, and then calculate the mean and std across all of the models to find the multi-model mean and std). All values are rounded to three significant figures.

S1.4 Calculating the Carbon Budget

Here we outline how we calculate the remaining carbon budget in both the linear mode and non-linear mode months. We first focus on the carbon budget to prevent a seasonally ice-free Arctic Ocean in the linear mode months. To quantify the remaining carbon budget in the linear mode months, we simply extract the cumulative CO_2 emission in the first year SIA falls below 1 million km^2. Whereas for those ensembles that do not reach 1 million km^2 by 2300, we interpolate over the linear period to diagnose the cumulative CO_2 emission at 1 million km^2, assuming the linear relationship persists. Additionally, SIA recovers in the low emission scenario (SSP1-2.6) due to its reliance on net negative CO_2 emissions, in particular on BECCS (biomass with carbon sequestration and storage). We therefore do not include ensembles that show SIA recovery in our analysis of the carbon budget in the linear mode months.

We estimate the threshold cumulative CO_2 emissions at which the rapid loss of Arctic sea ice occurs through the non-linear mode months by doubling the value of parameter 'b', as this provides the temperature of rapid SIA loss to Arctic warming. We first double the seasonal Arctic temperature dictated by 'b', then extract the year in which the seasonal Arctic temperature occurs in each non-linear mode month. From this, we then extract the MAGICC cumulative CO_2 emission at the same index, to determine the threshold CO_2 value at which rapid sea ice loss occurs. While the sensitivity of sea ice loss increases after this threshold, the relationship remains linear to ice-free conditions. We therefore calculate the sensitivity over the second linear period as the SIA loss per emitted ton of CO_2 that occurs between the threshold CO_2 emission of rapid ice loss, and the first time each ensemble drops below 1 million km^2. As the cumulative CO_2 emission projections begin in 1750, to analyse the remaining carbon budget from 2024 we simply subtract the cumulative CO_2 emission in 2024 from the total carbon budget in each ensemble.

As the scenarios SSP1-2.6 and SSP2-4.5 show significant emissions reductions, the temperature in the majority of ensembles in both scenarios does not rise significantly enough for sea ice to detach from land causing rapid ice loss. As such, we focus mainly on SSP5-8.5 when pinpointing this threshold. Within this scenario itself, a few ensembles do not reach ice-free conditions by 2300 due to the probabilistic nature of our observationally constrained Arctic Amplification. This is because there is the possibility of randomly sampling a cooler global mean temperature ensemble in combination with a small Arctic Amplification ensemble when calculating the Arctic annual mean temperature. In the ensembles that exhibit rapid ice loss but do not reach ice-free conditions by the simulations end, we estimate the sensitivity by interpolating over the available data. We therefore interpolate the sensitivity after rapid ice loss begins if the SIA continues to decline for at least 10 years after the sensitivity has increased. We therefore assume the constant linear decline of rapid ice loss holds until ice-free conditions occur. We find this to be sufficient as there is little year to year variability in the decline of SIA in our projections. The sensitivity over the 10 years after rapid ice loss begins is therefore also equal to the sensitivity 50 years after it begins.

Supplementary S2: Results

S2.1 Assessing the Performance of our Emulator to 2300

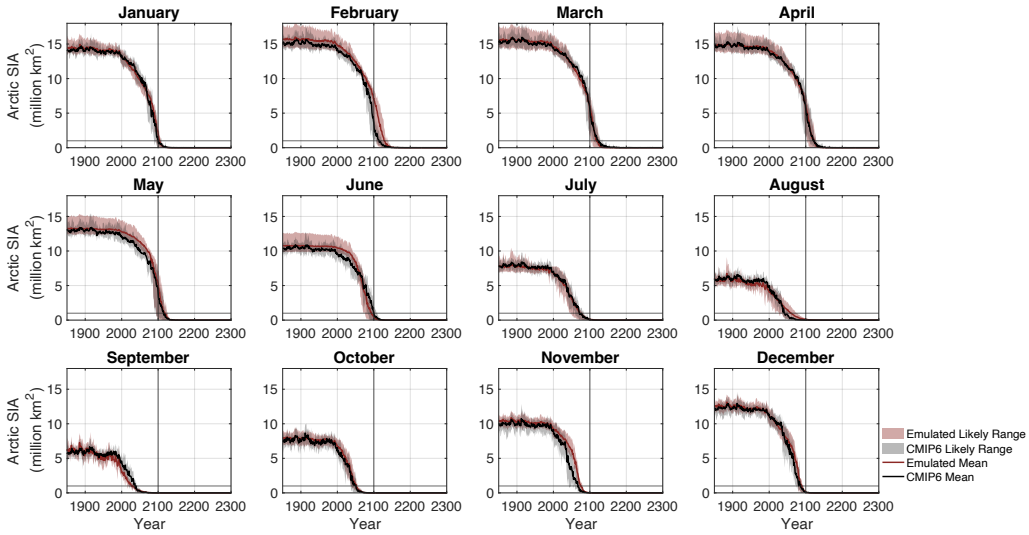

Figure S11. Emulated seasonal Arctic SIA between 1850-2300. Red shading represents the emulated SSP5-8.5 likely range from our CMIP6 emulator, while grey shading represents the SSP5-8.5 CMIP6 likely range. Red solid lines represent the emulated mean, and solid black line represents the CMIP6 multi-model median.

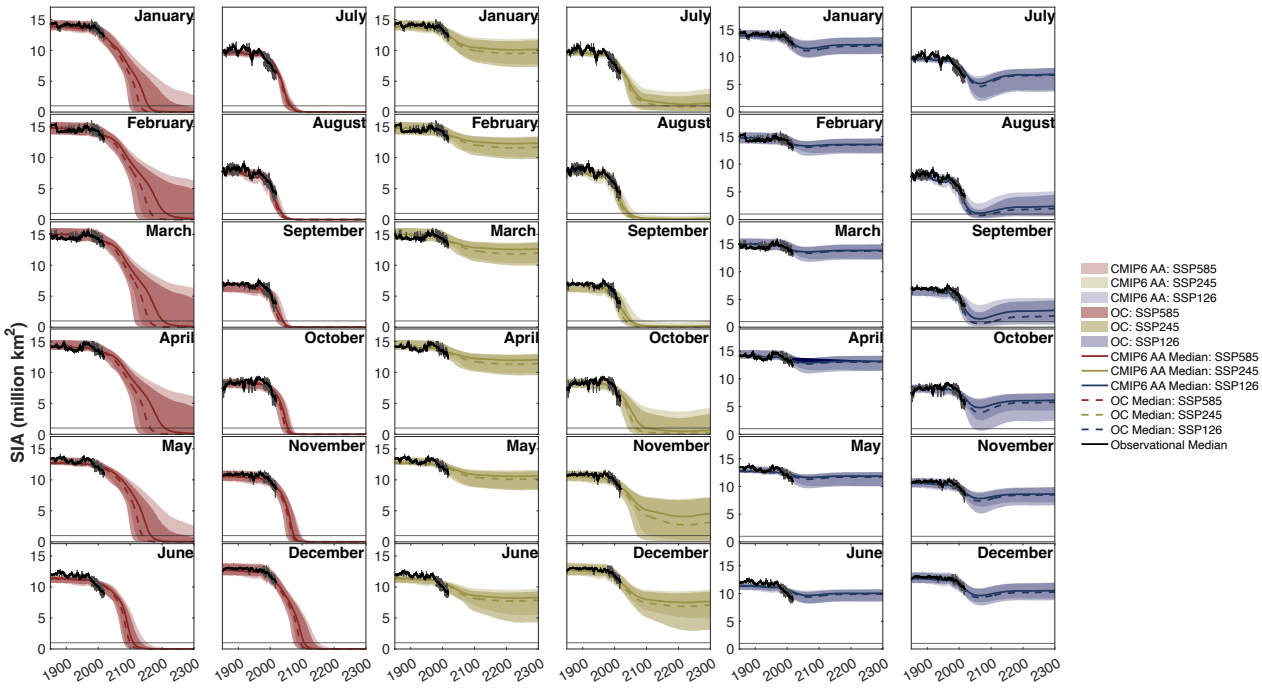

Figure S12. Emulated likely range of the monthly Arctic SIA over the time period 1850-2300 when our emulator is forced with the MAGICC 600-member ensemble global mean temperature anomaly. Red, yellow and blue shading represents SSP5-8.5, SSP2-4.5 and SSP1-2.6 respectively. Darker shading represents the projections from our observationally constrained emulator, and lighter shading represents the projections when forcing our emulator with the CMIP6 calibrated (linear) Arctic Amplification. The dashed and solid lines represent the mean SIA from each set of projections respectively. The black line spanning 1850-2020 represents observational data.

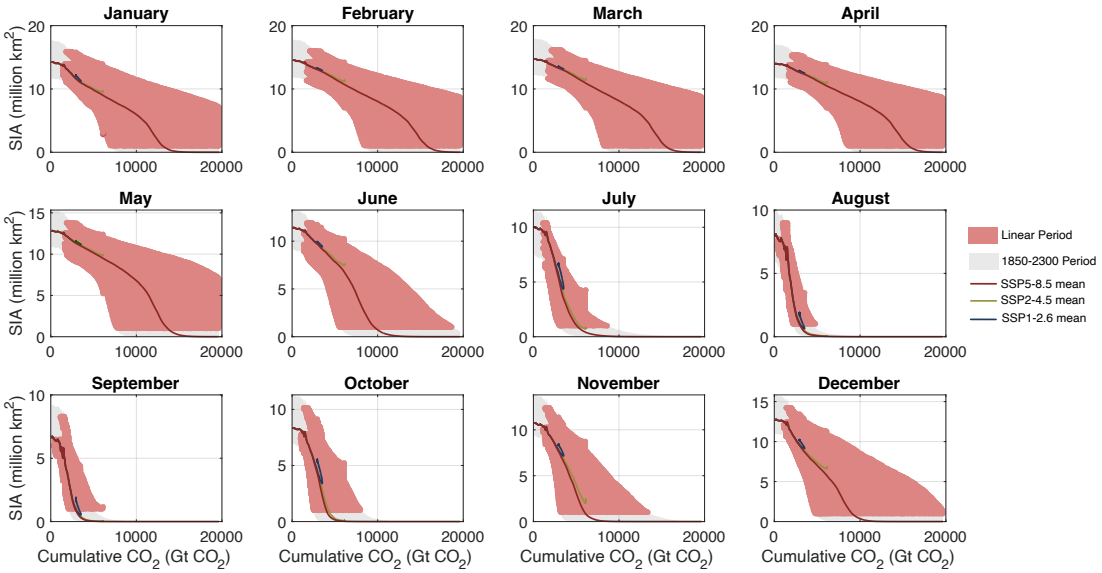

Figure S13. The seasonal decline of Arctic sea ice with cumulative CO_2 emissions. We highlight the difference between linear-mode (July-December) and non-linear mode months (January-June). Light red shading represents the SIA sensitivity to CO_2 emissions over the period between SIA falling below 10% of the pre-indsutrial mean and SIA reaching ice-free conditions ($<$1 million km^2). The 'linear period' is represented through dark red shading, while grey shading represents SIA outside of the 'linear period'. Red, yellow and blue solid lines represent the SSP5-8.5, SSP2-4.5 and SSP1-2.6 mean respectively.

SSPs	March		September	
	Year	GMST(°C)	Year	GMST(°C)
SSP5-8.5	2178	7.7	2037	1.89
SSP2-4.5	N/A	N/A	2046	1.89
SSP1-2.6	N/A	N/A	N/A	N/A

Table S5. Probability of a *likely* ice-free Arctic Ocean in September and March from our OC emulator. N/A implies the probability of an ice-free Arctic Ocean never becomes *likely* in this scenario.

S2.2 How Well Does Our CMIP6 Emulator Reproduce CMIP6 Data?

We calculate the likelihood of an ice-free Arctic Ocean occurring in each year as the ratio of the number of ensemble members projecting a SIA of 1 million km^2 or less in each year, to the total number of ensemble members used. Additionally, we calculate the probability of an ice-free ocean occurring at IPCC warming targets via a cumulative distribution function of the
590 global temperature at which sea ice falls below 1 million km^2 for the first time, across the multi-model ensemble. We make use of the IPCC likelihood scale where "*very unlikely*" equates to a probability of 0%–10%, "*unlikely*" equates to 10%–33%, "*as likely as not*" equates to 33%–66%, "*likely*" equates to 66%–90%, and "*very likely*" equates to 90%–100%. A 100% probability of an Arctic ice-free ocean is produced when the entire multi-model ensemble projects a SIA below 1 million km^2.

S2.3 How Well Does Our CMIP6 Emulator Reproduce CMIP6 Data?

We test the ability of our emulator to reproduce the CMIP6 Arctic Amplification, Arctic seasonal temperature and SIA response to global warming for the CMIP6 models used in the calibration process.

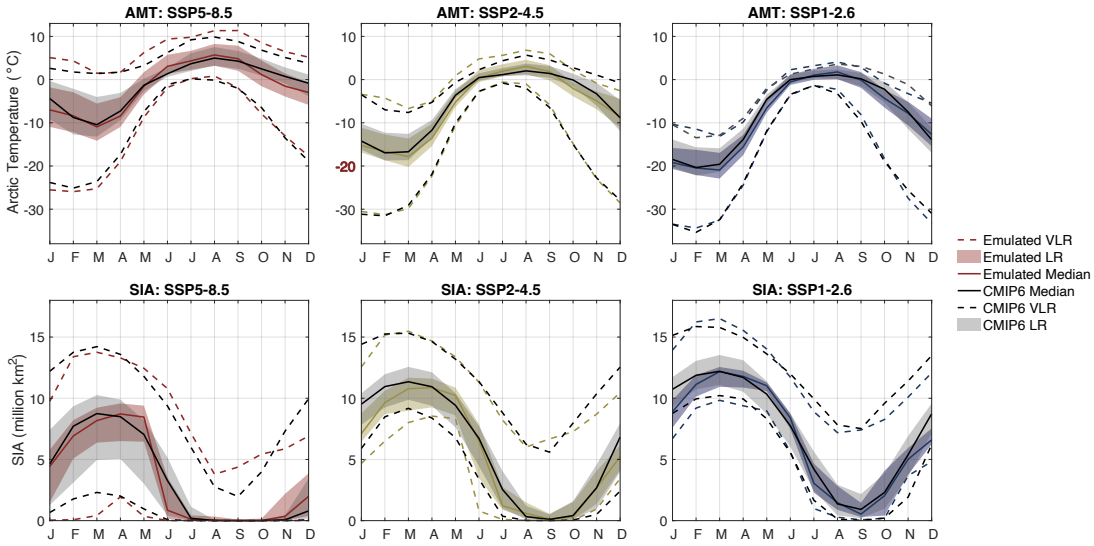

Figure S14. Comparison of our CMIP6 calibrated Arctic annual temperature cycle (top row) and Arctic SIA annual cycle (bottom row) from our CMIP6 calibrations with the equivalent CMIP6 range. Red, yellow and blue shading represents the 2080-2100 mean *likely* range from SSP5-8.5, SSP2-4.5 and SSP1-2.6 respectively. Grey shading represents the CMIP6 *likely* range. Solid red, yellow and blue lines represent the mean of our CMIP6 calibrated range. Dashed lines represent the CMIP6 calibrated *very likely* range.

When comparing the *likely* (17-83%) range of our emulated Arctic annual mean temperatures (stage i) with the *likely* range of their CMIP6 counterparts (fig. 2), it is clear a simple linear regression produces a relatively sufficient fit as all calibrated models and scenarios fall within the 95% confidence band of the CMIP6 counterpart.

Further statistical analysis shows that our emulator yields well calibrated parameter sets to replicate the CMIP6 seasonal Arctic temperature and SIA in SSP scenarios SSP1-2.6, SSP2-4.5 and SSP5-8.5 (fig. S14). The mean of the 2080-2100 CMIP6 multi-model distribution of the seasonal Arctic temperature cover the range -20.4°C (March) to 1.03°C (August), with a standard deviation range between 1.02 and 6.27 (Supplementary tables. S3 and S4). In comparison the sample mean produced from our emulation over the same period covers the range -20.9°C (March) to 1.12°C (August), with a standard deviation between 1.50 and 6.79. For our SIA parameterisation, our emulated mean covers the range 12.1 million km^2 at its maximum in March to 1.33 million km^2 at its minimum in September, with a standard deviation range between 2.34 and 1.49. The CMIP6 model distribution matches our emulation well with a range of mean SIA over this time between 12.4 million km^2 (March) and

1.51 million km^2 (September), with a standard deviation range between 2.42 and 1.45. Both ranges of the mean and standard deviation of our emulator significantly overlap their CMIP6 counterpart in both the temperature and SIA parameterisation, suggesting that our model's emulation is reasonably accurate in capturing the variability seen in the CMIP6 multi-model distribution. To evaluate the significance of the seasonal variances between our emulation of both variables and the CMIP6 counterpart, we use the Levene's test on the standard deviation of both the emulated and CMIP6 2080-2100 multi-model distribution (Supplementary tables. S3 and S4). When doing so we generate a p-value of 0.95 and 0.6, and an F-value of 0.0036 and 0.3 for our Arctic seasonal temperature and SIA emulations respectively.

The nuances between CMIP6 models suggest that our emulation of some models perform better than others in terms of how well they reproduce their CMIP6 counterpart. In both the seasonal temperature and SIA calibration, the models ACESSS_CM2 and CESM2 show a slightly degraded quality in terms of fit, especially in the month May. In general, we find May to be the worst fitting month in terms of both temperature and SIA, as our emulated May temperature does not increase as fast as its CMIP6 counterpart and therefore simulates too little SIA lost per degree of warming. When we remove May from our statistical evaluation, the p and F-values from our SIA projections change to 0.9 and 0.02 respectively, indicating a significantly increased fit when May is not accounted for. However overall, all other months fall within the 95% confidence band of the CMIP6 counterpart, when simply comparing the average 2080-2100, *very likely* (5-95%) and *likely* (17-83%) range. The emulated median of both variables also closely matches the CMIP6 counterpart with an R-squared value of 0.9, indicating our calibration produces a near-optimal emulation of the first ensemble CMIP6 multi-model range of all SSP scenarios.

S2.4 How well Our Emulator Reproduces Current Seasonal Temperature Trends?

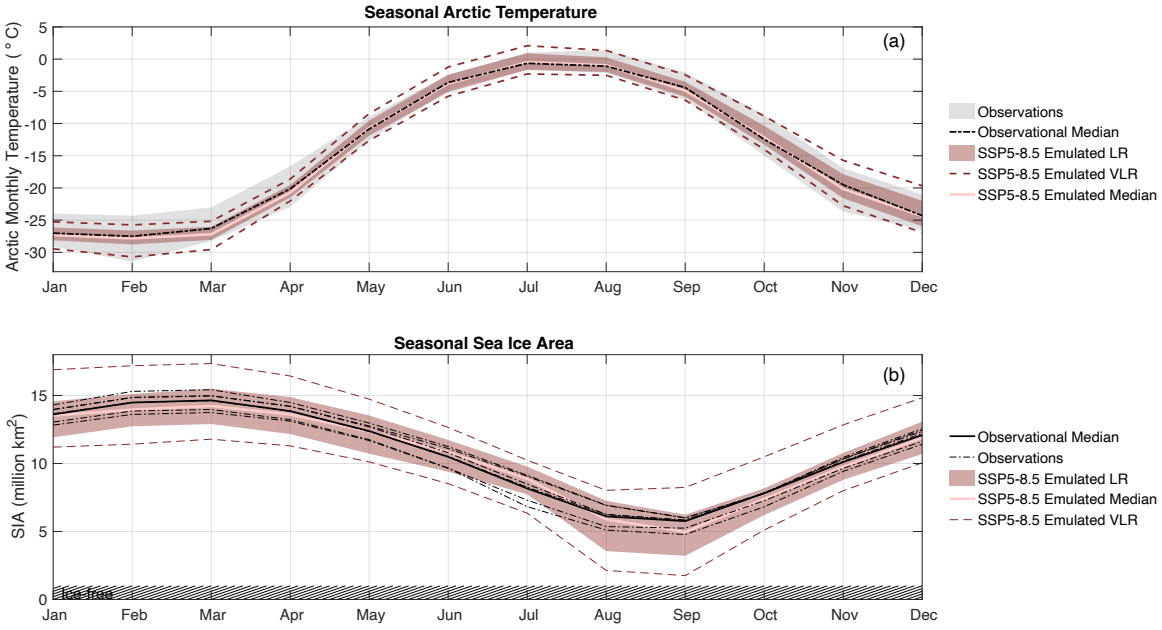

Figure S15. Comparison of our observationally constrained Arctic annual temperature cycle (top panel) and Arctic SIA annual cycle (bottom panel), with the 'plausible range' from observations. Red shading shows our calibrated 1979-2014 mean *likely* range. Dashed red lines denote the *very likely* calibrated range. Solid red lines denote the calibrated median. Grey shading represent the mean 1979-2014 *likely* range from observations. Dashed black lines denote individual observations and solid black lines denote the observational mean.

After constraining our emulator to observations, we find that our emulator is able to sufficiently capture the observed Arctic seasonal temperature cycle, when comparing the 1979-2014 *very likely* (5-95%) and *likely* (17-83%) emulated range with the observed (fig. S15). The unconstrained median 1979-2014 temperature cycle shows a positive bias between January and August with temperatures on average 1.92°C higher than the observed over this time (fig. S16). After applying the observational constraints, these biases reduce to 0.063°C, where the observed and constrained median Arctic seasonal temperature cycle show an R-squared correlation of 0.98 and an RSS goodness of fit value of 0.0636. When specifically comparing the emulated July and August temperatures to the observed, we find that after adding the bias corrections to our temperature parameterisation Eq. (2b), our summer temperatures increase at the same rate as the observed median. We therefore find that our projections reproduce the observational Arctic warming in all months, within the 95% confidence of observations.

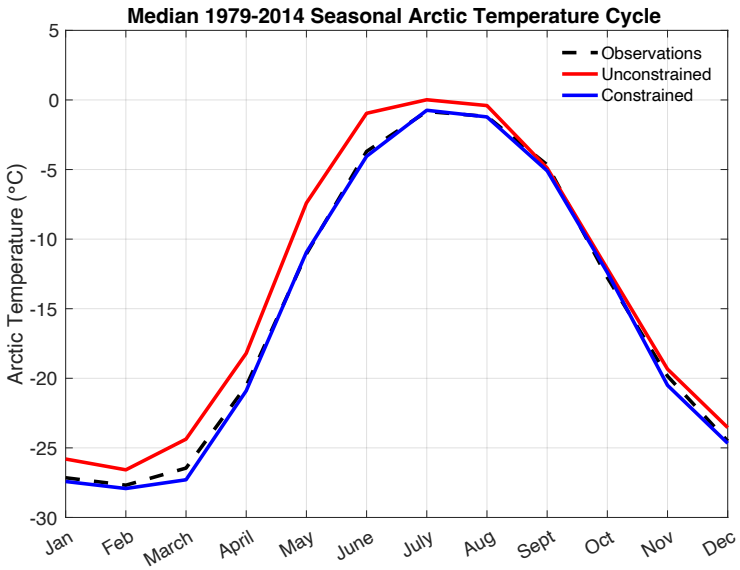

Figure S16. Comparison of the median 1979-2014 observationally constrained seasonal Arctic temperature cycle with our unconstrained CMIP6 calibrated median 1979-2014 seasonal Arctic temperature cycle. Red solid lines represent our unconstrained CMIP6 calibration, blue solid lines represent our observationally constrained emulator and black dashed lines show its comparison to observations.